JOURNAL OF GEOPHYSICAL RESEARCH, VOL. 111, D12310, doi:10.1029/2005JD006663, 2006

Black carbon measurement in a coastal area of south China

Y. Cheng,[1] S. C. Lee,[1] K. F. Ho,[1] Y. Q. Wang,[2] J. J. Cao,[3] J. C. Chow,[4] and J. G. Watson[4]

Received 12 September 2005; revised 20 November 2005; accepted 23 March 2006; published 23 June 2006.

[1] To better understand anthropogenic pollution originating in Asia and its transport into the global atmosphere, black carbon (BC) emissions were measured continuously from June 2004 to May 2005 at Hok Tsui (22.13°N, 114.15°E). Hok Tsui is a continental outflow, downwind monitoring site, located in a coastal area near Hong Kong. Using an Aethalometer, hourly BC concentrations ranged from 63.0 ng/m^3 to 17.3 μg/m^3, showing a clear seasonal pattern with high concentrations in winter, spring, and fall and low values in summer. During the winter, high BC concentrations occurred frequently as a result of southward long-range transport of polluted air masses in the boundary layer over the Asian continent. Anthropogenic emissions in coastal areas of southeastern China were the major potential sources for the observed pollutants. During the summer, high BC concentrations were measured occasionally when the air masses came from the northwest. These anthropogenic pollutants were found to be regional in nature, originating from sources in the Pearl River Delta (PRD) region, which included emissions from residential and agricultural combustion, industry, power plants, motor vehicles, and ships.

Citation: Cheng, Y., S. C. Lee, K. F. Ho, Y. Q. Wang, J. J. Cao, J. C. Chow, and J. G. Watson (2006), Black carbon measurement in a coastal area of south China, *J. Geophys. Res.*, *111*, D12310, doi:10.1029/2005JD006663.

1. Introduction

[2] Black carbon (BC) is an anthropogenic aerosol that significantly warms the atmosphere through absorption of solar radiation [*Schult et al.*, 1997; *Jacobson*, 2001]. Second only to CO_2, in terms of direct climate forcing, BC is believed to be a principal component of global warming since its warming effect has been found to balance the net cooling effect of other anthropogenic aerosol constituents [*Haywood and Shine*, 1995; *Jacobson*, 2001]. Most past research on BC has been conducted in regions outside of Asia, but a few recent studies within Asia show the importance of BC on that continent. *Streets et al.* [2001] estimated that BC emissions in China (1342 Gg in 1995 and 1224 Gg in 2020), represent ~30% of global anthropogenic emissions. *Bond et al.* [2004] have produced similar findings. *Köhler et al.* [2001] suggested that BC particles from road traffic in Asia cause direct radiative forcing three times higher than European road traffic. Another study conducted recently by NASA (National Aeronautics and Space Administration) found that about one-third of the soot observed in the atmosphere over the Arctic comes from southern Asia [*Koch and Hansen*, 2005]. The region is considered the world's largest source of industrial soot emissions.

[3] Other past studies [*Cao et al.*, 2003; *Ho et al.*, 2003; *Wang et al.*, 1997, 2001, 2003; *Cohen et al.*, 2004; *Louie et al.*, 2005a] have investigated the influence of regional and long-range transport of aerosols in the atmosphere of Hok Tsui, which is located downwind of east Asia and China. There, the southward outflow of continental pollution prevails in the lower atmosphere during fall, winter and early spring. *Wang et al.* [1997, 2001, 2003] conducted intensive studies from February to April 2001 to characterize the chemical properties of the southward outflow of continental pollution from China. Chemicals that were characterized included ozone (O_3), CO, NO, NO_y, SO_2, ^{222}Rn, methane (CH_4), and C_2–C_8 nonmethane hydrocarbons, C_1–C_2 halocarbons, and C_1–C_5 alkyl nitrate. They found that differences in chemical constituents were influenced by emission changes and meteorological variation. *Cohen et al.* [2004] investigated BC mass concentrations at Hok Tsui every Wednesday and Sunday morning during an 18-month period from 2001 to 2002 and found mean BC mass concentration to be 2.3 ± 1.7 μg/m^3. Black carbon on the Teflon filters was estimated by measuring the transmission of (He/Ne) laser light (wavelength 0.633 nm) through the filters before and after exposure. *Louie et al.* [2005a] explored the meteorological characteristics on $PM_{2.5}$ (particles less than 2.5 μm in diameter) mass and chemical composition by collecting 24-hour interval $PM_{2.5}$ samples every sixth day at Hok Tsui from 5 November 2000 to 26 October 2001. Air parcel back trajectory and residence time analysis showed that southeastern China and western Taiwan were potential $PM_{2.5}$ sources during winter and fall

[1]Department of Civil and Structural Engineering, Hong Kong Polytechnic University, Kowloon, Hong Kong.
[2]Centre for Atmosphere Watch and Services, Chinese Academy of Meteorological Sciences, Beijing, China.
[3]State Key Laboratory of Loess and Quaternary Geology, Institute of Earth Environment, Chinese Academy of Sciences, Xi'an, China.
[4]Division of Atmospheric Sciences, Desert Research Institute, Reno, Nevada, USA.

0148-0227/06/2005JD006663

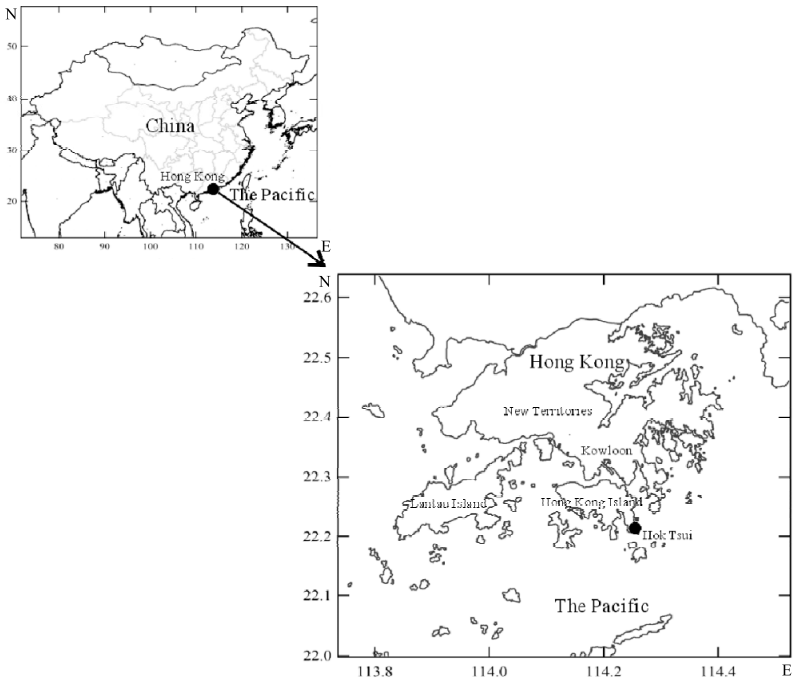

Figure 1. Sampling location, Hok Tsui.

and the regional pollution episodes resulted from a combination of synoptic-scale monsoon and mesoscale subsidence with moderate to stagnant easterly transport.

[4] Although these studies begin to more accurately portray the presence and role of BC in the atmosphere of east Asia, few anywhere have made continuous measurements and few have sufficiently focused on source determination of southward outflows of Asian pollution. Lack of this fundamental information on Asian BC has resulted in great uncertainty in the simulation of black carbon distribution and its corresponding contribution to global climate change [*Schult et al.*, 1997; *Haywood and Shine*, 1995; *Chung and Seinfeld*, 2005]. The purpose of this paper is three-fold: to report findings from hourly, monthly, and yearly BC averages from June 2004 to May 2005 at Hok Tsui; to trace the major outflow pathways and transport mechanisms for southward export of Asian anthropogenic emissions, using BC as a tracer, with the hybrid single-particle Lagrangian integrated trajectories (HYSPLIT) model [*Draxler and Hess*, 1998]; and to determine the potential source contribution for southward outflow of Asian pollution with a statistical method of potential source contribution function (PSCF). In order to provide comparable BC data, we first determined the site-specific cross section for Aethalometer measurements by comparing BC results from the optical and thermal-optical methods.

2. Methodology

2.1. Measurement Site

[5] The Hok Tsui (HT) atmospheric research station was established in 1993 at the southeastern tip of Hong Kong Island where it faces the South China Sea at an elevation of 60 m above sea level (Figure 1). Since no major emission sources are located in the sampling site's vicinity, measurements at Hok Tsui are expected to have "background" atmospheric properties, which are determined largely by the transport of air masses from upwind.

2.2. BC Measurements

[6] A model AE-42 Aethalometer (Magee Scientific Inc., Berkeley, Calif.) with a $PM_{2.5}$ inlet was used to measure aerosol BC in real time from 4 June 2004 to 31 May 2005. The Model AE-42 is a portable unit that embodies all of the standard Aethalometer features. It measures optical absorption at 880 nm for particles deposited on the 1.6 cm^2 quartz-fiber filter (PALL Corp., New York). The Aethalometer was placed at 1.5 m above ground and operated at 5 l/min.

[7] The Aethalometer measures the attenuation of a beam of light ($ATN_{(\lambda)}$) transmitted through a filter, as particles are collected on the filter. The instrument has two photodetectors. One, *RB* (reference beam), measures the intensity of light that crosses a "clean" spot of quartz filter; the other, *SB* (sensing beam), measures the intensity of the same light that crosses the sample spot where the aerosol is continuously accumulating. The Aethalometer also measures the signals at the sensors when the light source is turned off (*RZ* for the reference beam and *SZ* for the sensing beam). These values are subtracted from the sensors' levels when the light source is turned on in order to correct the measurements from the dark currents. The attenuation is defined as

$$ATN_{(\lambda)} = -100 \times \ln((SB - SZ)/(RB - RZ)) \qquad (1)$$

where the factor of 100 is introduced for numerical convenience. By using the appropriate value of the specific attenuation cross section ($\sigma_{(1/\lambda)}$), the black carbon content of

the aerosol deposit can be determined at each timebase cycle, as follows:

$$BC = \frac{ATN(T) - ATN(0)}{\sigma_{(1/\lambda)}} \times \frac{A}{V} \quad (2)$$

where $ATN(0)$ and $ATN(T)$ are the initial and the final attenuations due to the aerosol deposit on the filter during each timebase cycle; A (m^2) is the area of the exposed spot on the filter; and V (m^3) is the volume of air drawn through the filter. The BC minimum detection limit (MDL) is below 10 ng/m^3 for the Aethalometer AE-42 used in this study. This is the standard deviation in small fluctuations determined by sampling filtered air in a cleaning room with the Aethalometer for 8 hours. All data measured at Hok Tsui have higher concentrations than the MDL. BC data were subsequently averaged to a time resolution of 1 hour in order to be aligned with meteorological data and other studies.

2.3. Determination of Specific Attenuation Cross Section

[8] The specific attenuation cross section ($\sigma_{(1/\lambda)}$) is the most important parameter for optical BC determination using an Aethalometer [*Petzold et al.*, 1997]. This attenuation is proportional to BC mass concentration [*Rosen et al.*, 1980]. It changes with age, type, and composition of aerosols, which vary with time and space [*Sharma et al.*, 2002]. This is primarily due to other particle-bound material accompanying BC, such as soil, sulfate, water, organics, etc. [*Hansen et al.*, 1984]. Thus the attenuation cross section values of 16.6 m^2/g used in the Aethalometer by the manufacturer may need to be adjusted when the greatest accuracy is required for a given site.

[9] According to equation (2), the aerosol's optical attenuation ($ATN_{(\lambda)}$) during each timebase cycle is a product of BC mass concentration and attenuation cross section:

$$ATN_{(\lambda)} = BC \times \sigma_{(1/\lambda)} \quad (3)$$

The real attenuation cross section for a specific time period can be estimated from the ratio of the Aethalometer BC to a corresponding elemental carbon (EC) measurement by the thermal optical analysis of a collected filter sample [*Petzold et al.*, 1997; *Sharma et al.*, 2002]. Although optical and thermal methods have contradictory limitations in their use, such as multiple reflection of a light beam and modification of refraction of black carbon on a quartz filter during Aethalometer measurement [*Liousse et al.*, 1993], and charring of organic particulate in thermal analysis [*Yu et al.*, 2002], thermal analyses are believed to directly provide more reasonable results than the optical method before the true site-specific cross section is determined for the Aethalometer [*Liousse et al.*, 1993]. It should be noted that all techniques for BC, including that of the Aethalometer, are essentially method-dependent. Different methods provide results derived from different attributes of the carbonaceous aerosol material.

[10] For comparison, time-integrated $PM_{2.5}$ samples were collected, in parallel with the Aethalometer, at 24-hour interval on quartz-fiber filters (QMA, Whatman International Ltd., Maidstone, UK, 47mm in diameter) with a Plus Model 2025 Sequential Air Sampler (Rupprecht and Patashnick Co. Inc., Albany, N. Y.) at Hok Tsui. The flow rate was 16.7 l/m. The quartz-fiber filters were preheated at 900° C for 3 hours to reduce blank levels. The carbonaceous content was determined using a Desert Research Institute (DRI) Model 2001 Thermal/Optical Carbon Analyzer (AtmAA Inc, Calabasas, Calif.) with the IMPROVE thermal optical reflectance (TOR) protocol [*Chow et al.*, 1993, 2004]. Almost all samples in this study had concentrations higher than the MDL. The MDL of carbon combustion methods is 0.19 μg/cm^2 for EC. Replicate analyses were performed for ~10% of all samples to estimate precision. Field blanks were collected to correct EC concentrations on the filters. The TOR protocol proved more suitable for analyzing Hong Kong aerosol samples than the thermal optical transmittance (TOT) protocol [*Chow et al.*, 2005].

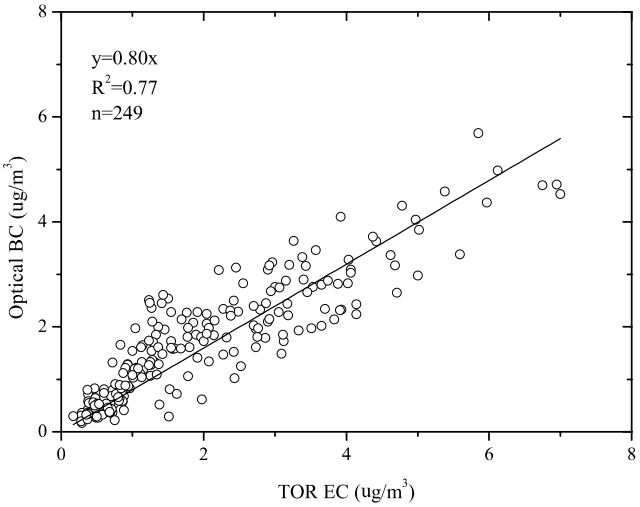

Figure 2. Comparison of 24-hour average black carbon (BC) mass concentrations between the Aethalometer and TOR method; n is the number of sampling days.

[11] The comparison between the Aethalometer BC data and the TOR EC data were performed, as shown in Figure 2. The 5-min Aethalometer BC data were averaged into 24-hour values temporally matching the 249 EC data derived from in-parallel, filter-based samples. In Figure 2, the attenuation cross-section of 16.6 m^2/g for Aethalometer was used to calculate the optically derived BC concentration. Good relationship is found between the Aethalometer and TOR measurements, with a high correlation coefficient of 0.77 (R^2), indicating that they respond similarly. The BC concentrations derived from the Aethalometer were ~20% lower than TOR measurements. These results provide the information needed to adjust the attenuation cross section (σ_{abs}) in equation (1) so that BC determined by Aethalometer agrees with BC determined from the TOR technique.

[12] The calculated attenuation cross sections varied from sample to sample at Hok Tsui with a median of 15 m^2/g, which is lower compared to roadside measurements in Hong Kong (17 m^2/g, unpublished) and in Paris (19 m^2/g [*Ruellan and Cachier*, 2000]). The variability of cross sections is

Table 1. Statistic Summary From Hourly Average Black Carbon Mass Concentrations From June 2004 to May 2005

Season	n[a]	Mean, μg/m^3	Standard Deviation, μg/m^3	Minimum, μg/m^3	Maximum, μg/m^3
Summer	2812	1.4	1.6	0.1	13.4
Fall	1464	2.9	1.8	0.1	12.1
Winter	2849	3.0	1.7	0.4	17.5
Spring	1464	2.5	1.5	0.3	13.3
Total	8589	2.4	1.8	0.1	17.5

[a]Number of hours.

believed to be due to coating and aging of the particles and to the variability of the aerosol mixture [*Liousse et al.*, 1993].

3. Results

3.1. BC Mass Concentrations

[13] The yearly means for this study were evaluated from hourly average BC data collected by Aethalometer, using the determined specific attenuation coefficient. Measured from June 2004 to May 2005 (Table 1), annual average BC concentration at Hok Tsui was 2.4 ± 1.8 μg/m^3. This is comparable to previous studies conducted by *Cohen et al.* [2004], with a mean of 2.3 ± 1.7 μg/m^3, and *Louie et al.* [2005b], with a mean of 2.0 ± 0.9 μg/m^3. *Cohen et al.* [2004] estimated $PM_{2.5}$ BC by measuring the transmission of (He/Ne) laser light (wavelength 0.633 nm) through Teflon filters before and after exposure, while *Louie et al.* [2005b] determined $PM_{2.5}$ EC concentrations on quartz filters using the IMPROVE TOR protocol. Throughout the sampling period, the lowest 1-hour BC value was 63.0 ng/m^3 in summer, which is quite similar with the EC concentrations (68–71 ng/m^3) observed in the central North Pacific Ocean measured by the thermal/combustion technique [*Kaneyasu and Murayama*, 2000]. A seasonal variation of BC was obvious, with the highest monthly average in January (4.1 ± 2.3 μg/m^3) and the lowest in July (1.0 ± 1.3 μg/m^3) (Figure 3). The average BC concentration during the winter was more than twice that of summer (Table 1).

[14] The contribution of BC from different wind directions is illustrated by the pollution roses in Figure 4. As can be seen, BC loadings during sampling period increased when surface winds were from the north/northeast/east (0–105 degree). Hourly BC concentrations from this sector were in the 2–7 μg/m^3 range, much higher than the 1–2 μg/m^3 from the southwest. Since mainland China lies north of Hong Kong, high BC levels are most likely due to the influence of continental aerosols that transported from the mainland by the northeast monsoon, which is generated by the cooling and heating of the great Asian land mass. During the sampling period, more than ~70% of surface winds were from the northeast with average wind speeds exceeding 6 m/s. As Figure 4 shows, northerly/northeasterly winds usually prevailed in fall, winter, and spring, corresponding with relatively high BC concentrations during these seasons. In contrast, during the summer only ~28% of the surface winds came from the northeast. Southerly and northwesterly winds occurred for ~60% and ~12% of summer season, respectively. BC concentrations were 1–2 μg/m^3 when southerly winds dominated, indicating that the air masses bring relative clean marine aerosols to Hok Tsui. High BC concentrations (3–10 μg/m^3), averaging of 3.3 ± 2.7 μg/m^3, were observed when the winds from the northwest, Guangdong Province, although only ~12% of winds came from this sector.

3.2. BC Events

[15] Figure 5 displays the temporal patterns of hourly BC from June 2004 to May 2005. The diurnal patterns were found to be variable during the study period. Morning peaks usually observed during traffic rush hours at urban sites were not observed at Hok Tsui, implying that contributions from the local major source in Hong Kong, namely vehicle exhausts, were negligible at this sampling location. It was noted that the hourly BC data showed some events in which concentrations increased greatly for periods of a few hours to a few days. Extremely high BC concentrations were clearly evident during these events with BC concentrations exceeding 7 μg/m^3 (Figure 5). Since there are no stable sources continuously emitting BC near the sampling location, except for occasional ship emissions, those events should reflect regional or long-range transport pollution. In order to identify the meteorological characteristics and typical transport mechanisms for these events, we first scanned the hourly BC data in order to pick up the "BC event," which was defined as periods when hourly BC concentrations exceeded 7 μg/m^3 within a continuous 4-hour timeframe. These criteria resulted in a somewhat subjective selection of events from the available record, but we expect that this will make the BC events more representative.

[16] Table 2 shows the time and date of BC events during the study period, along with corresponding meteorological

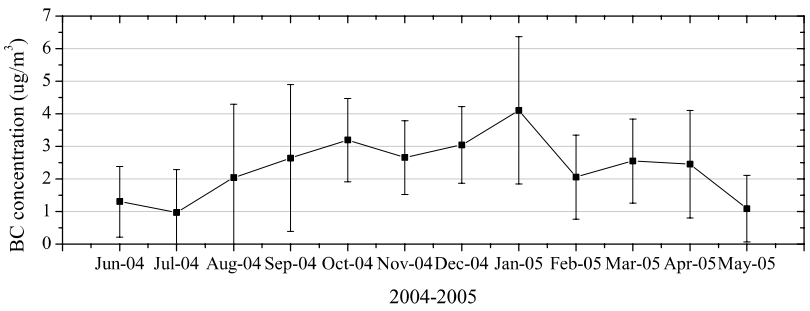

Figure 3. Monthly average BC concentrations; the bar represents one standard deviation of hourly averages.

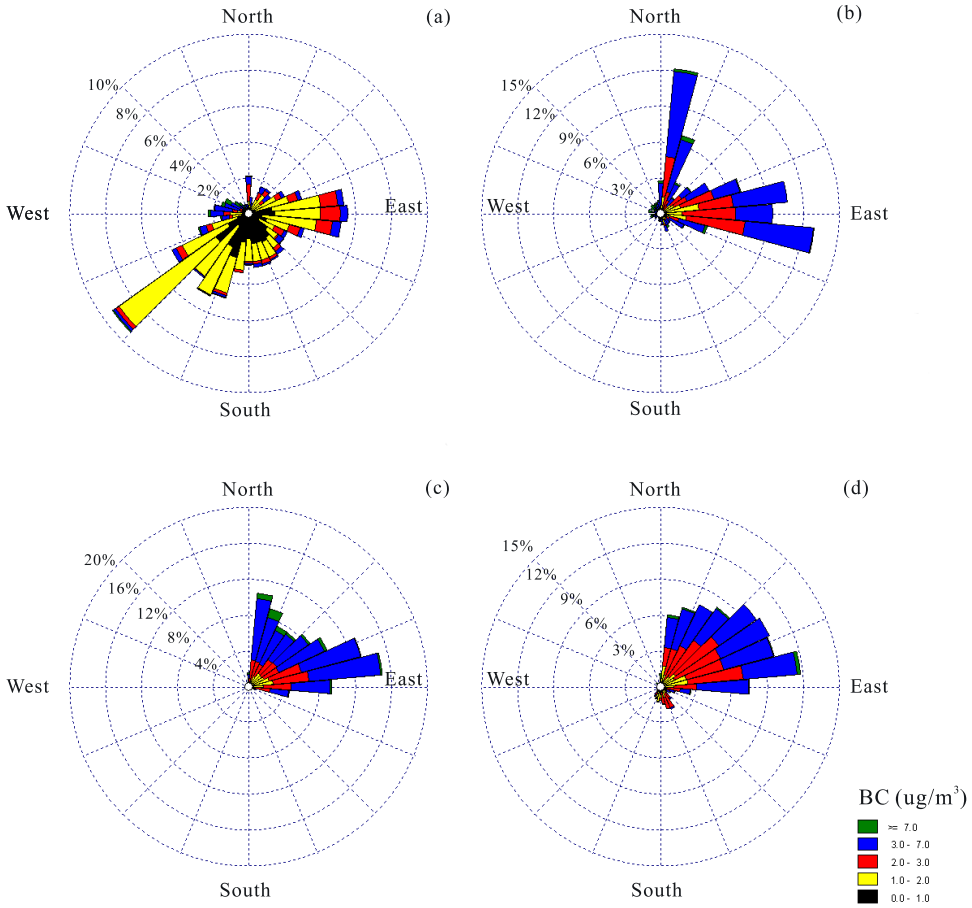

Figure 4. Pollution roses of hourly average BC in (a) summer, (b) fall, (c) winter, and (d) spring.

records and mixing heights. Except for summer, the northeasterly winds were dominant for all seasons; while in summer northwesterly winds prevailed during BC events. Wind speeds were usually low, with an average of 2.8 m/s for all events, compared to the average of 5.9 m/s for the entire sampling period. Meanwhile, mixing heights generally showed lower values during BC events than overall average mixing heights of 1064 m. All of these are evidence

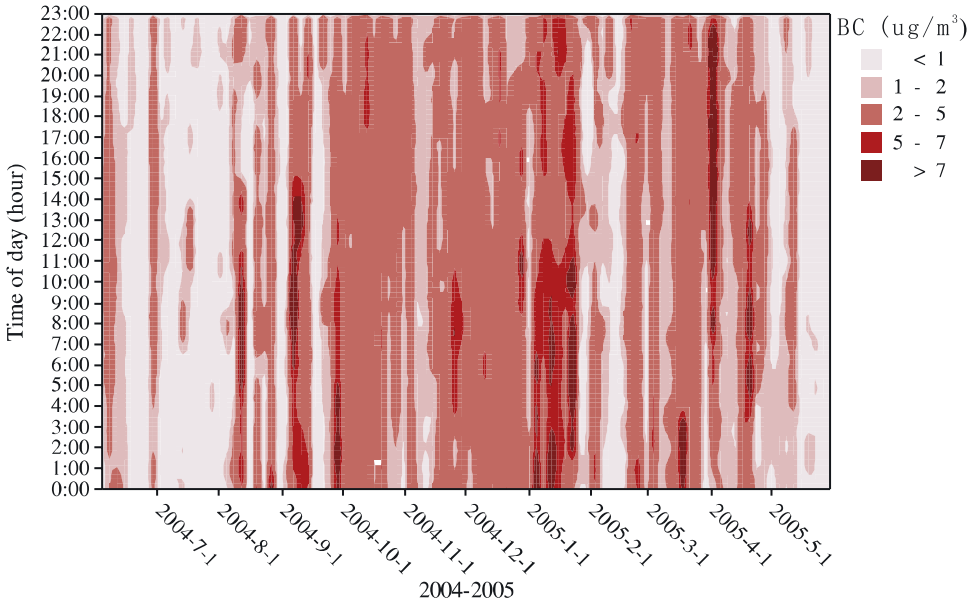

Figure 5. Temporal patterns of BC from June 2004 to May 2005.

Table 2. Meteorological Observations During BC Events From June 2004 to May 2005

Season	Date	Hours	BC, μg m^{-3}	WS,[a] m s^{-1}	WD,[b] °C	Pres,[c] hPa	MH,[d] m	Synoptic Conditions[e]
Summer	27 Jul 2004	1100–1600	11.3	3	307	1002	974	An area of low pressure over the northern part of the South China Sea intensified into a tropical depression on the early morning of 27 July.
	12 Aug 2004	0500–1000	10.1	3.4	305	1002	560	After a ridge of high pressure, the weather was fine after 7 August, turning cloudy with some thunder showers on 11 and 12 August.
	17 Aug 2004	1400–1800	11.7	5.3	267	1002	687	It was mainly fine and hot during 15 to 18 Aug. It was hot and hazy with light winds on 18 and 19 August. Visibility dropped to below 1000 m in parts of the territory.
	18 Aug 2004	1800–2200	10.5	1.5	310	1002	947	
	24 Aug 2004	0900–1600	11.1	2.5	250	1003	515	Thunderstorm and very hot weather warning.
	25 Aug 2004	0300–0800	9.5	3.5	328	1000	2078	Typhoon Aere skirts the northern part of Taiwan.
Fall	6 Sep 2004	0900–1400	11.6	0.1	10	1003	909	Associated with Typhoon Songda in the East China Sea, a trough of low pressure formed over the coast of Guangdong and brought thunder showers to the area on 6 September.
	7 Sep 2004	0600–0900	9.6	1.3	28	1004	842	Associated with Typhoon Songda in the East China Sea, a trough of low pressure persisted over the coast of Guangdong.
	15 Sep 2004	0300–2000	9.8	2	106	1008	1033	A dry continental airstream arrived at the coast on 10 September. Generally fine weather continued during the next 5 days.
	16 Sep 2004	0300–1400	9.3	0.9	33	1012	1064	Under light wind conditions, it was hazy on 15 and 16 September with the visibility falling to below 2000 m in parts of the territory.
	28 Sep 2004	0100–0500	10.9	2.7	312	1011	2238	The continental airstream behind the cold front dominated over southern China. The weather remained generally fine.
Winter	4 Jan 2005	0000–1000	14.1	3.5	8	1020	447	An intense surge of the winter monsoon brought fine, dry and very cold weather to Hong Kong on the first day of January. While remaining cold, it turned cloudy on 2 and 3 January with the weakening of the winter monsoon.
	6 Jan 2005	0300–1900	9.5	3.5	43	1020	500	The weather turned fine on 6 January after the winter monsoon.
	10 Jan 2005	0000–1400	8.9	7.3	35	1022	732	Generally, fine weather prevailed after the winter monsoon. There were long periods of haze from 4 to 12 January.
	12 Jan 2005	0000–0700	10.2	5.3	13	1022	795	
	23 Jan 2005	0200–1100	11.9	2.5	30	1020	1912	Under the influence of a maritime airstream, it was humid with mist and fog in Hong Kong from 23 to 30 January.
Spring	2 Apr 2005	0800–2200	9.8	2.3	348	1015	523	It is fine and dry weather on 2 April when a northeast monsoon arrived at the south China coast.
	20 Apr 2005	0500–0900	8	0.6	18	1017	613	With plenty of sunshine, it was hot with maximum temperatures exceeding 30°C in the New Territories on 20 April.

[a]Wind speed.
[b]Wind direction.
[c]Pressure.
[d]Mixing height.
[e]Note the synoptic conditions are available at http:www.hko.gov.hk/wxinfo/pastwx/mws.htm.

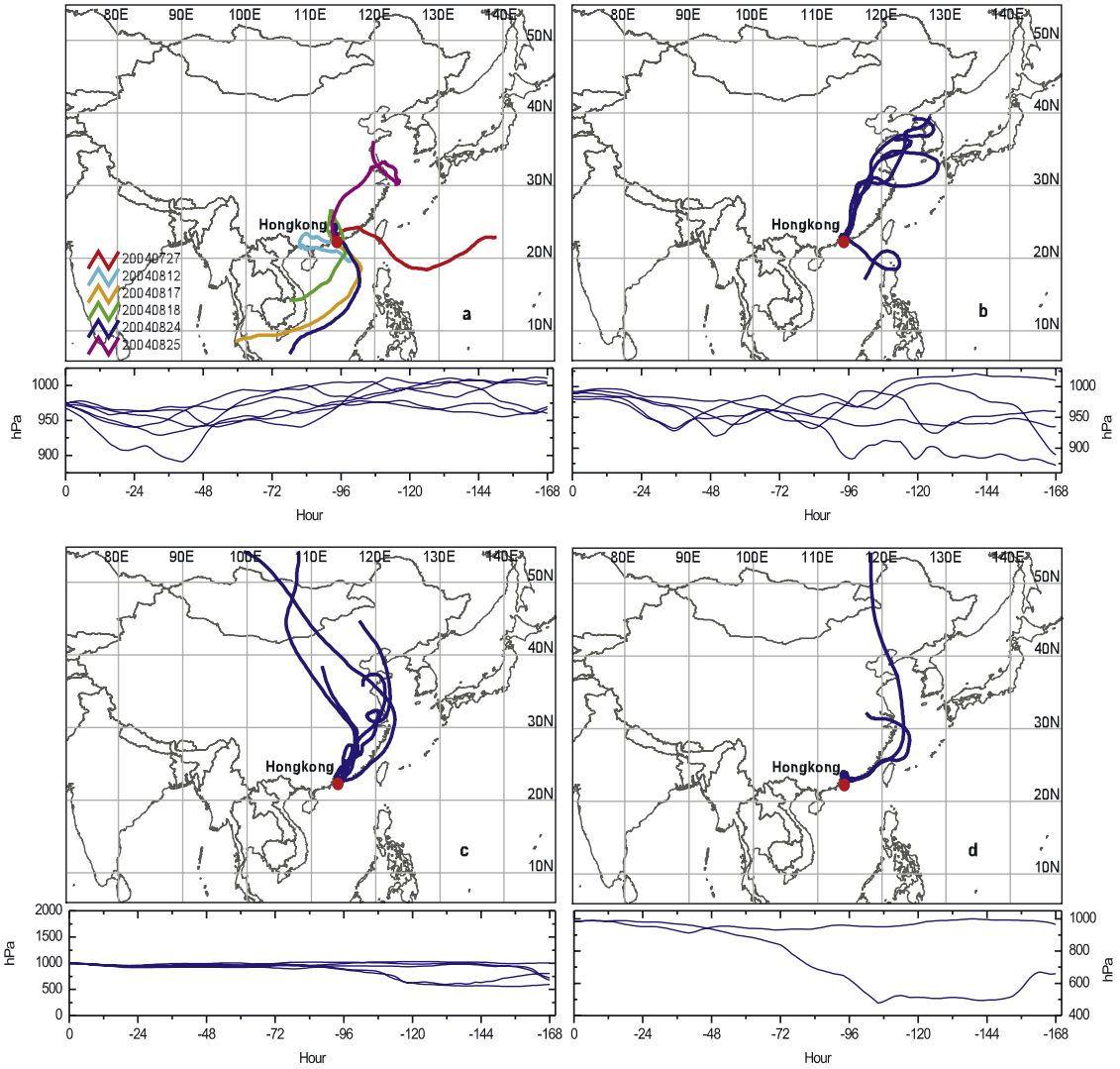

Figure 6. Seven-day air mass back trajectories during 18 BC events in (a) summer, (b) fall, (c) winter, and (d) spring.

of poor dispersion conditions during BC events, as also observed by *Louie et al.* [2005a]. Other meteorological parameters (e.g., temperature, pressure, and relative humidity) showed less difference between BC event days and nonevent days.

3.3. Southward Outflow of Asian Pollution in Winter, Spring, and Fall

[17] To investigate the southward outflow regimes for anthropogenic aerosols, the hybrid single-particle Lagrangian integrated trajectories (HYSPLIT) model [*Draxler and Hess*, 1998] was used to trace the 7-day back trajectories using BC as a marker for the BC events in Table 2.

[18] Figure 6 shows 7-day back trajectories arriving at 150 m above the Hok Tsui sampling site for each BC event. All BC events corresponded with the continental outflow of anthropogenic emissions to the Pacific. Only five BC events were recorded during the winter of 2004–2005, which was not considered an average year meteorologically, because the year 2004 in Hong Kong was the ninth warmest on record, and the northeast monsoon during the last 2 months of the year was weak, giving rise to warmer and fewer cold fronts than expected at year end (available at http://www.hko.gov.hk/wxinfo/pastwx/ywx2004.htm). Presumably, if the weather were more what is considered typical, more BC events with greater BC concentrations would occur. As shown in Figure 6c, in most cases when high concentrations of BC were measured in winter, air parcels arriving at Hok Tsui had traveled a long distance over the Asian continent: from Mongolia, through Inner Mongolia in northern China, across the Hua Bei Plain, on toward coastal areas in eastern China, then southward to Hong Kong along the coastal line. The outflow pathway represented typical cold fronts over the Asian continent during winter [*Chin*, 1986], which are triggered by the extension of the Siberian anticyclone southeastward over China [*Ding*, 1990]. This transport is confined to the lower troposphere and recurs with a frequency of 2–7 days in normal conditions.

[19] Table 2 shows that a cold front was often recorded several days before a winter BC event. The event usually

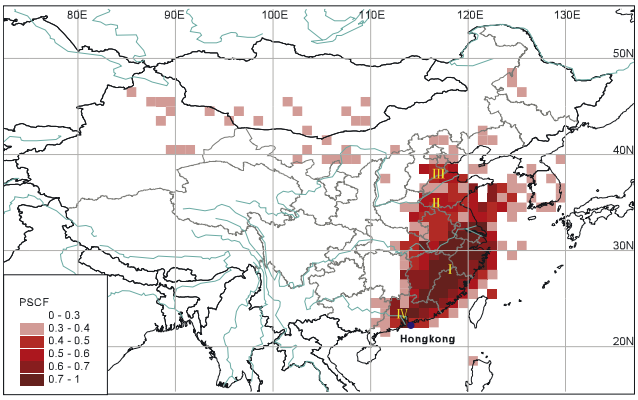

Figure 7. PSCF map for southward outflow of anthropogenic aerosols in 2004–2005.

occurred with a cold high pressure system, clear skies, and a light northeasterly wind. *Liu et al.* [2003] investigated the outflow resulting from cold surges over Hong Kong from 1 February to 15 April 2001. He observed ~10 cold surges, during which, two types of outflow were observed: one was the carbon monoxide (CO) frontal outflow in free troposphere (FT) ahead of the front, with similar contributions of anthropogenic and biomass burning emissions; the other was the boundary layer (BL) continental outflow behind the front, capped at an altitude of ~2 km and accompanied by strong subsidence. The latter outflow contained high pollutant concentrations with CO levels in excess of 250 ppbv and was largely devoid of biomass burning contributions that were identified in the first type. Obviously, the outflow pattern corresponding to BC events in this study is associated with the transport in the BL behind cold fronts.

[20] The main outflow patterns in the fall (Figure 6b) and spring (Figure 6d) are similar to those for winter except for the relatively weak intensity of cold surges, which produces short transport distances of the air masses over the Asian continent. This is because the cold high pressure is in either its initial or late phase during these seasons.

3.4. Southward Outflow of Asia Pollution in Summer

[21] During the summer, two major outflow pathways were observed (Figure 6a). Besides the one similar to that in fall that occurred at the end of summer (25 August), the other represents the most common summertime case when a hot air mass generated over the tropical maritime moves northward inland. We noticed that disturbances caused an important shift in the direction of the air masses at the border of Guangdong Province, where air parcels turned back toward the southeast. Typically, during summer, a large semipermanent depression develops over the southwestern provinces of China that brings warm and moist southerly or southwesterly winds over Hong Kong [*Ding*, 1994]. However, the summer monsoon is much less prominent than its winter counterpart and is frequently interrupted when the depression is replaced by the south Asia high (Tibetan anticyclone) [see *Chin*, 1986, Figure 3.5]. This interruption might explain why the northward marine air stream was obstructed and turned toward the southeast. This is supported by previous modeling results [*Liu et al.*, 2003], which show that the pollution may frequently lifted into the upper troposphere by deep convection when the summer monsoonal flow moves northward from the Pacific Ocean to the Asian continent. In the upper troposphere a large fraction of upswelled Asian pollution circulates southward and then westward around the south Asia high, resulting in outflow toward the Middle East.

[22] During the transport of air masses over the PRD region, which is the most developed region in south China, a large number of pollutants were introduced into the air parcels that would be expected to be clean, given its marine origins. Thus the highest BC concentrations in summer are often observed when the northwestern surface wind prevails at Hok Tsui. This result is consistent with the pollution rose analysis of Figure 4.

3.5. Potential Source Contribution to Air Pollution at Hok Tsui

[23] Potential source contribution function (PSCF) is a statistical method that evaluates the source contribution of air pollution at a receptor site by counting trajectory segment endpoints that terminate within each cell [*Ashbaugh*, 1983; *Wang et al.*, 2004]. The PSCF value for a single grid cell is a normalized value that can be calculated as follows:

$$PSCF_{ij} = m_{ij}/n_{ij} \tag{4}$$

where m_{ij} is the number of endpoints for ijth cell having times of arrival at the sampling site corresponding to pollutant concentrations higher than a selected value. n_{ij} means the number of all endpoints that fall in the same cell. Cells with high PSCF values indicate that the regions are high potential contributions to the pollution at the receptor site. In this study the selected value is set to the mean concentration of all BC data (2.4 $\mu g/m^3$).

[24] In order to evaluate the potential source contribution to air pollution in the atmosphere of Hok Tsui, the PSCF values were calculated based on a total of 362 7-day back-trajectories arriving at Hok Tsui at 1200 (local time) of each day from 4 June 2004 to 31 May 2005. According to the results of the PSCF analysis (Figure 7), four potential source areas were identified as having important contributions to BC at Hok Tsui. Source area I was coastal portion of southeastern China, including the Yangtze River Delta region, and Jiangxi, Zhejiang, and Fujian Province. Source area II was the region between Hebei and Shandong Province. Source area III was on the border between Shangdong and Henan Province. The PRD region constituted source area IV.

[25] *Streets et al.* [2003] developed a BC emission inventory for China in 2000, which included all major anthropogenic sources and biomass burning. As reported by *Streets et al.* [2001, 2003], BC emissions in China were dominated by the residential sector (~74%) and were concentrated in a west-to-east swath curving across the agricultural heartland of China from Sichuan Province to Hebei Province [see *Streets et al.*, 2001, Figure 1]. Most air masses arriving at Hok Tsui do not travel over the major documented BC emission source areas in China. Although

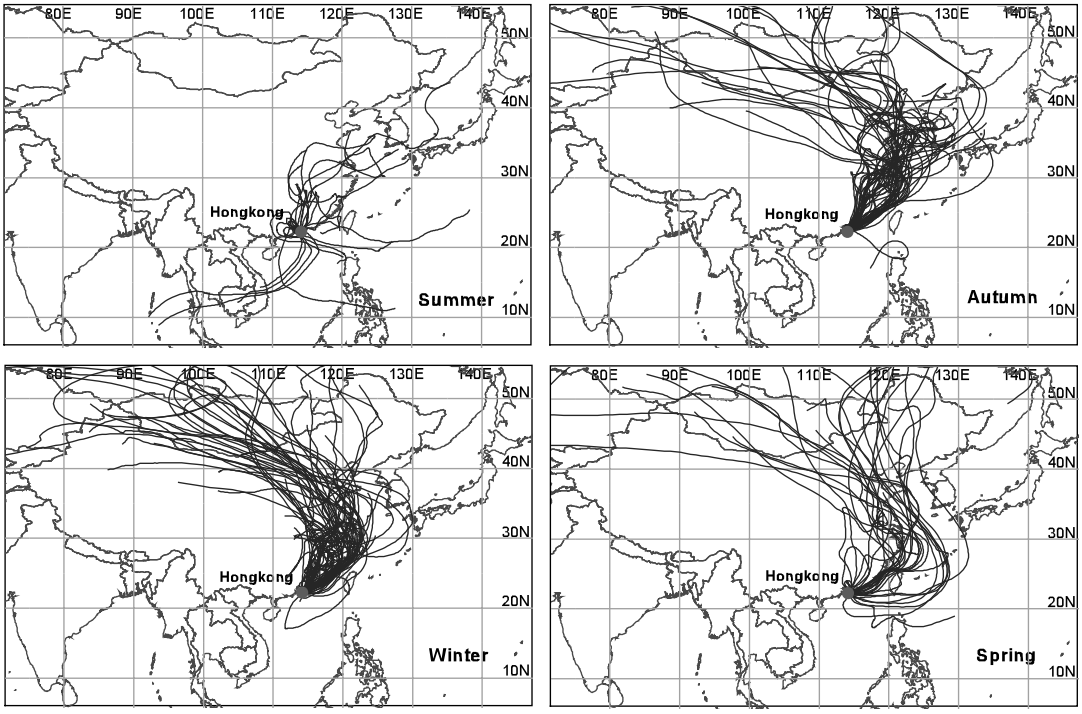

Figure 8. Seven-day air mass back trajectories during those days with the BC concentrations exceeding the mean value in summer, fall, winter, and spring.

source areas II and III identified in the present study are located in the boundary zone of the important BC emission areas, few of polluted air mass trajectories directly pass through these regions, as shown in Figure 8. BC emissions in source areas I and IV have more effectively influence on the BC in Hong Kong than source areas II and III because most polluted air parcels arriving at Hok Tsui travel over source area I in winter, spring, and fall, and travel over source area IV in summer.

[26] Rapid industrialization in southeastern China (source area I) in recent years implies its significance as a long-range transport source in the future. Energy consumption in southeastern China is expected to increase dramatically and BC emissions are predicted to increase from 1996 to 2050, particularly due to the transportation sector [*Streets et al.*, 2004]. Hok Tsui, as a receptor, may experience higher BC levels from long-range transport sources in winter, spring, and fall if effective control strategies are not implemented.

[27] The PRD region (source area IV) is an important regional source area for pollutants observed at Hok Tsui in summer. Residential coal and biofuel combustion were the dominant BC emitters in 1995 [*Streets et al.*, 2001], accounting for ~65% of total emitted BC in PRD region. Agricultural burning and other activities made up ~5% and ~30%, respectively. ''Other activities'' include motor vehicles, industrial emissions, and power plants (available at http://www.epd.gov.hk/epd/english/environmentinhk/air/studyrpts/study_pearl.html). In the Hong Kong area, high BC emissions associate with the traffic emissions at roadside sites [*Louie et al.*, 2005a] and marine ship emissions near the port [*Yu et al.*, 2004]. BC arriving at Hok Tsui in summer is a mixture from residential and agricultural combustion, industry, power plants, motor vehicles, and ship emissions from the PRD region (including Hong Kong).

4. Conclusions

[28] BC measurements were conducted with an Aethalometer at Hok Tsui from June 2004 to May 2005. The BC comparisons between the Aethalometer and the IMPROVE TOR method showed day-to-day variability in the specific attenuation cross section. Aethalometer BC mass concentrations in the present study were adjusted using the reconstructed specific attenuation cross section of 15 m^2/g, as a result of the comparisons.

[29] The annual average BC concentration at Hok Tsui was 2.4 ± 1.8 $\mu g/m^3$, which is comparable to levels found in previous studies by other measurement methods. Throughout the sampling period, the minimum 1-hour BC value was 63.0 ng/m^3 in summer, also similar to levels in clean air over the central north Pacific Ocean. The highest monthly BC concentration occurred in January (4.1 ± 2.3 $\mu g/m^3$) and the lowest in July (1.0 ± 1.3 $\mu g/m^3$).

[30] Northeasterly winds usually prevailed in fall, winter, and spring, corresponding to relatively high BC concentrations of 2–7 $\mu g/m^3$, due to the influence of continental aerosols transported from mainland China. During the summer, ~28% of the surface winds were from the northeast, ~60% of the winds from the south, and ~12% from the northwest. BC concentrations were 1–2 $\mu g/m^3$ when southerly winds dominated, indicating that the southern air masses bring relatively clean marine aerosols to Hok Tsui. High BC concentrations (3–10 $\mu g/m^3$) were observed when

the winds were from the northwest, with an average BC concentration of 3.3 ± 2.7 μg/m^3.

[31] During the winter, air parcels arriving at Hok Tsui traveled from Mongolia, through Inner Mongolia in northern China, across Hua Bei Plain toward the eastern China coast, then southward along the coastline to Hong Kong. The outflow pathway represents typical cold surges over the continent of Asia, which is an episodic incursion of cold midlatitude air that is triggered by the extension of the Siberian anticyclone southeastward over China. The episodes are confined to the lower troposphere and recur with a frequency of 2–7 days in normal conditions. The outflow pattern corresponding to BC events associates with the transport of air masses in the boundary layer behind cold surges. During the summer, however, a hot air mass, generated over tropical ocean waters, first moved northward inland, then, intercepted by a newly established South Asia high across southwestern China Provinces, turned back to southeast near the border of Guangdong Province, and finally entered Hong Kong from the northwest. These air masses brought considerable pollutants to Hok Tsui, although it traveled extremely short distances over the mainland.

[32] Using back trajectories corresponding to those days with high BC concentrations, four potential air pollution source areas were identified. Source area I was the coastal region in southeastern China. Source area II was the region between Hebei and Shandong Province. Source area III was located on the border areas of Shangdong and Henan Province, and source area IV was PRD region. Most air masses arriving at Hok Tsui do not travel over the major BC emission source regions in China. The BC emissions in source areas I and IV have more influence on BC in Hong Kong than source areas II and III because most polluted air parcels travel over source area I in winter, spring, and fall, and travel over source area IV only in summer.

[33] **Acknowledgments.** We would like to acknowledge the general support from the PolyU Atmospheric Research Station, Hong Kong Polytechnic University. This research was supported by Hong Kong Polytechnic University and Research Grants Council of Hong Kong (PolyU 5197/05E and PolyU 5145/03E) and the Area of Strategic Development on Atmospheric and Urban Air Pollution (A516) funded by the Hong Kong Polytechnic University.

References

Ashbaugh, L. L. (1983), A statistical trajectory technique for determining air pollution source regions, *J. Air Pollut. Control. Ass.*, *33*, 1096–1098.

Bond, T. C., D. G. Streets, K. F. Yarber, S. M. Nelson, J.-H. Woo, and Z. Klimont (2004), A technology-based global inventory of black and organic carbon emissions from combustion, *J. Geophys. Res.*, *109*, D14203, doi:10.1029/2003JD003697.

Cao, J. J., S. C. Lee, K. F. Ho, X. Y. Zhang, S. C. Zou, K. Fung, J. C. Chow, and J. G. Watson (2003), Characteristics of carbonaceous aerosol in Pearl River Delta Region, China during 2001 winter period, *Atmos. Environ.*, *37*, 1451–1460.

Chin, P. C. (1986), Climate and weather, in *A Geography of Hong Kong*, edited by T. N. Chiu and C. L. So, pp. 69–85, Oxford Univ. Press, New York.

Chow, J. C., J. G. Watson, L. C. Pritchett, W. R. Pierson, C. A. Frazier, and R. G. Purcell (1993), The DRI Thermal/optical reflectance carbon analysis system: description, evaluation and applications in U.S. air quality studies, *Atmos. Environ.*, *27A*(8), 1185–1201.

Chow, J. C., J. G. Watson, L. W. A. Chen, W. P. Arnott, H. Moosmüller, and K. Fung (2004), Equivalence of elemental carbon by thermal/optical reflectance and transmittance with different temperature protocols, *Environ. Sci. Technol.*, *38*(16), 4414–4422.

Chow, J. C., J. G. Watson, P. K. K. Louie, L. W. A. Chen, and D. Sin (2005), Comparison of $PM_{2.5}$ carbon measurement methods in Hong Kong, China, *Environ. Poll.*, *137*(2), 334–344.

Chung, S. H., and J. H. Seinfeld (2005), Climate response of direct radiative forcing of anthropogenic black carbon, *J. Geophys. Res.*, *110*, D11102, doi:10.1029/2004JD005441.

Cohen, D. D., D. Garton, E. Stelcer, O. Hawas, T. Wang, S. Poon, J. Kim, B. C. Choi, S. N. Oh, H.-J. Shin, M. Y. Ko, and M. Uematsu (2004), Multielemental analysis and characterization of fine aerosols at several key ACE-Asia sites, *J. Geophys. Res.*, *109*, D19S12, doi:10.1029/2003JD003569.

Ding, Y. H. (1990), Build-up, air mass transformation and propagation of the Siberian High and its relation to cold surge in East Asia, *Meteorol. Atmos. Phys.*, *44*, 281–292.

Ding, Y. H. (1994), *Monsoons Over China*, Springer, New York.

Draxler, R. R., and G. D. Hess (1998), An overview of the HYSPLIT-4 modeling system for trajectories, description, and deposition, *Aust. Meteorol. Mag.*, *47*, 295–308.

Hansen, A. D. A., H. Rosen, and T. Novakov (1984), The aethalometer-an instrument for the real-time measurement of optical absorption by aerosol particles, *Sci. Total Environ.*, *36*, 191–196.

Haywood, J. M., and K. P. Shine (1995), The effect of anthropogenic sulfate and soot aerosol on the clear sky planetary radiation budget, *Geophys. Res. Lett.*, *22*, 603–606.

Ho, K. F., S. C. Lee, C. K. Chan, J. C. Yu, J. C. Chow, and X. H. Yao (2003), Characterization of chemical species in $PM_{2.5}$ and PM_{10} aerosols in Hong Kong, *Atmos. Environ.*, *37*, 31–39.

Jacobson, M. Z. (2001), Strong radiative heating due to the mixing state of black carbon in atmospheric aerosols, *Nature*, *409*, 695–697.

Kaneyasu, N., and S. Murayama (2000), High concentrations of black carbon over middle latitudes in the North Pacific Ocean, *J. Geophys. Res.*, *105*(D15), 19,881–19,890.

Koch, D., and J. Hansen (2005), Distant origins of Arctic black carbon: A Goddard Institute for Space Studies Model experiment, *J. Geophys. Res.*, *110*, D04204, doi:10.1029/2004JD005296.

Köhler, I., M. Dameris, I. Ackermann, and H. Hass (2001), Contribution of road traffic emissions to the atmospheric black carbon burden in the mid-1990s, *J. Geophys. Res.*, *106*(D16), 17,997–18,014.

Liousse, C., H. Cachier, and S. G. Jennings (1993), Optical and thermal measurements of black carbon aerosol content in different environments: Variation of the specific attenuation cross-section, sigma (σ), *Atmos. Environ.*, *27A*(8), 1203–1211.

Liu, H., D. J. Jacob, I. Bey, R. M. Yantosca, B. N. Duncan, and G. W. Sachse (2003), Transport pathways for Asian pollution outflow over the Pacific: Interannual and seasonal variations, *J. Geophys. Res.*, *108*(D20), 8786, doi:10.1029/2002JD003102.

Louie, P. K.-K., J. G. Watson, J. C. Chow, L.-W. A. Chen, D. W.-M. Sin, and A. K.-H. Lau (2005a), Seasonal characteristics and regional transport of $PM_{2.5}$ in Hong Kong, *Atmos. Environ.*, *39*(9), 1695–1710.

Louie, P. K.-K., J. C. Chow, A. Chen, J. G. Watson, G. Leung, and D. W.-M. Sin (2005b), $PM_{2.5}$ chemical composition in Hong Kong: Urban and regional variations, *Sci. Total Environ.*, *338*, 267–281.

Petzold, A., C. Kopp, and R. Niessner (1997), The dependence of the specific attenuation cross-section on black carbon mass fraction and particle size, *Atmos. Environ.*, *31*(5), 661–672.

Rosen, H., A. D. A. Hansen, R. L. Dod, and T. Novakov (1980), Soot in urban atmosphere: Determination by an optical absorption technique, *Science*, *208*, 741–743.

Ruellan, S., and H. Cachier (2000), Characterization of fresh particulate vehicular exhausts near a Paris high flow road, *Atmos. Environ.*, *35*, 453–468.

Schult, I., J. Feichter, and W. F. Cooke (1997), Effect of black carbon and sulfate aerosols on the global radiation budget, *J. Geophys. Res.*, *102*(D25), 30,107–30,118.

Sharma, S., J. R. Brook, H. Cachier, J. Chow, A. Gaudenzi, and G. Lu (2002), Light absorption and thermal measurements of black carbon in different regions of Canada, *J. Geophys. Res.*, *107*(D24), 4771, doi:10.1029/2002JD002496.

Streets, D. G., S. Gupta, S. T. Waldhoff, M. Q. Wang, T. C. Bond, and Y. Y. Bo (2001), Black carbon emissions in China, *Atmos. Environ.*, *35*, 4281–4296.

Streets, D. G., et al. (2003), An inventory of gaseous and primary aerosol emissions in Asia in the year 2000, *J. Geophys. Res.*, *108*(D21), 8809, doi:10.1029/2002JD003093.

Streets, D. G., T. C. Bond, T. Lee, and C. Jang (2004), On the future of carbonaceous aerosol emissions, *J. Geophys. Res.*, *109*, D24212, doi:10.1029/2004JD004902.

Wang, T., K. S. Lam, L. Y. Chan, and A. S. Y. Lee (1997), Trace gas measurements in coastal Hong Kong during the PEM-West B, *J. Geophys. Res.*, *102*, 28,575–28,588.

Wang, T., T. F. Vincent, K. S. Lam, G. L. Kok, and J. M. Harris (2001), The characteristics of ozone and related compounds in the boundary layer of the South China coast: Temporal and vertical variations during autumn season, *Atmos. Environ.*, *35*, 2735–2746.

Wang, T., A. J. Ding, D. R. Blake, W. Zahorowski, C. N. Poon, and Y. S. Li (2003), Chemical characterization of the boundary layer outflow of air pollution to Hong Kong during February–April 2001, *J. Geophys. Res.*, *108*(D20), 8787, doi:10.1029/2002JD003272.

Wang, Y. Q., X. Y. Zhang, R. Arimoto, J. J. Cao, and Z. X. Shen (2004), The transport pathways and sources of PM10 pollution in Beijing during spring 2001, 2002, and 2003, *Geophys. Res. Lett.*, *31*, L14110, doi:10.1029/2004GL019732.

Yu, J. Z., J. H. Xu, and H. Yang (2002), Charring characteristics of atmospheric organic particulate matter in thermal analysis, *Environ. Sci. Technol.*, *36*, 754–761.

Yu, J. Z., J. W. T. Tung, A. W. M. Wu, A. K. H. Lau, P. K. K. Louie, and J. C. H. Fung (2004), Abundance and seasonal characteristics of elemental and organic carbon in Hong Kong PM_{10}, *Atmos. Environ.*, *38*(10), 1511–1521.

J. J. Cao, State Key Laboratory of Loess and Quaternary Geology, Institute of Earth Environment, Chinese Academy of Sciences, Xi'an, 710071, China.

Y. Cheng, K. F. Ho, and S. C. Lee, Department of Civil and Structural Engineering, Hong Kong Polytechnic University, Hung Hom, Kowloon, 000000, Hong Kong. (ceslee@polyu.edu.hk)

J. C. Chow and J. G. Watson, Division of Atmospheric Sciences, Desert Research Institute, 2215 Raggio Parkway, Reno, NV 89512, USA.

Y. Q. Wang, Centre for Atmosphere Watch and Services, Chinese Academy of Meteorological Sciences, 46, Zhong-Guan-Cun South Avenue, Beijing, 100081, China.